EFDA–JET–CP(10)04/06

R.C. Pereira, A.M. Fernandes, A. Neto, J. Sousa, C.A.F. Varandas, J. Cardoso, C.M.B.A. Correia, M. Tardocchi, M. Nocente, G. Gorini, V. Kiptily, B. Syme, M. Jennison and JET EFDA contributors

Pulse Analysis for Gamma-Ray Diagnostics ATCA Sub-Systems of JET Tokamak

Pulse Analysis for Gamma-Ray Diagnostics ATCA Sub-Systems of JET Tokamak

R.C. Pereira[1], A.M. Fernandes[1], A. Neto[1], J. Sousa[1], C.A.F. Varandas[1], J. Cardoso[2], C.M.B.A. Correia[2], M. Tardocchi[3], M. Nocente[3], G. Gorini[3], V. Kiptily[4], B. Syme[4], M. Jennison[4] and JET EFDA contributors*

JET-EFDA, Culham Science Centre, OX14 3DB, Abingdon, UK

[1]Associação EURATOM/IST Instituto de Plasmas e Fusão Nuclear- Laboratório Associado, Instituto Superior Técnico, Universidade Técnica de Lisboa, 1049-001 Lisboa, Portugal
[2]Grupo de Electrónica e Instrumentação do Centro de instrumentação, Dept. de Física, Universidade de Coimbra, 3004-516 Coimbra, Portugal.
[3]EURATOM-ENEA-CNR Association Instituto di Fisica del Plasma, Milan, Italy
[4]EURATOM-UKAEA Fusion Association, Culham Science Centre, OX14 3DB, Abingdon, OXON, UK
** See annex of F. Romanelli et al, "Overview of JET Results", (Proc. 22 nd IAEA Fusion Energy Conference, Geneva, Switzerland (2008)).*

Preprint of Paper to be submitted for publication in Proceedings of the 17th IEEE NPSS Real Time Conference, Lisbon, Portugal.
(24th May 2010 - 28th May 2010)

ABSTRACT.

A new Data Acquisition (DAQ) sub-system for gamma-ray diagnostics was developed for Joint European Torus (JET). The system is based on the ATCA platform and is able to sample up to 400 MSPS with 14-bit resolution. This DAQ is used for gamma-ray diagnostics dedicated to the study of fast ions in fusion tokamak plasma experiments. The present work describes the development of pulse processing algorithms used to extract the pulse parameters from the DAQ free running ADC data streams. These algorithms are divided in three main functional blocks, namely, advanced triggering and segmentation, segmentation validation and finally, peak height analysis (PHA) and Pile-Up Rejection (PUR).

The developed algorithms perform the pulse segmentation, shaping and validation according to the noise level and characteristics of the digitized signal. Shaping is performed through a reconfigurable trapezoidal filter in order to optimize the spectral resolution with the required throughputs and a comprehensive study of this parameterization is presented. Calibration procedures are mandatory for an efficient real time application and its implementation in the FPGA is discussed and explained.

The presented and discussed results refer to the analysis of the JET pulse files obtained during the recent campaigns where a spectral resolution of 4.5% for the ^{137}Cs energy peak at 662keV was achieved through FPGA real time processing. Results of high

1. INTRODUCTION

The Joint European Torus (JET) Gamma-ray diagnostics are increasingly demanding from the point of view of current data acquisition (DAQ) systems, both due to the larger number of detectors and the high rate of occurrence of relevant events. Moreover, DAQ systems will play a key role when orchestrating diagnostics data from very long-duration plasma discharges, as achieving long-duration, high-performance discharges in magnetic fusion devices is one of the most important challenges faced by fusion reactors [1].

New DAQ systems must be designed with high processing capabilities in order to provide high throughputs as well as the capability of storing significant data throughout the time of the experience to fully exploit the flux increase of the plasma provided by future high power experiments at JET and ITER [2].

This paper presents some results from the two JET's gamma-ray diagnostics: gamma-ray cameras and gamma-ray spectroscopy (GRS).

1.1. GAMMA-CAMERA

The present setup has two arrays of collimators (10 horizontal and 9 vertical lines of sight). Each line of sight has 3 detector systems based on scintillators tailored at different energies: i) NE213 liquid scintillator with pulse shape discriminator electronics (2.5MeV and 14MeV n/γ emission); ii) BC418 plastic scintillator (14MeV); iii) CsI(Tl) scintillator (0.2-6MeV γ emission measurements).

Only one of these detectors will be looking directly to the plasma. The present setup is called the neutron/fast-electron-bremsstrahlung (FEB)/gamma profile monitor. The present gamma-camera system profiles accommodate the γ-ray count-rate measurement in four independently adjustable energy windows. These energy windows allow the determination of the emission profile from the plasma and the tomographic reconstructions of the spatial distribution of gamma emission during Ion Cyclotron Resonance Heating (ICRH) JET pulse discharges. Programming the energy windows is a cumbersome process and cannot be done between discharges, as changing the experience parameters has to be performed at an analogical setup. Signal to noise ratio at the diagnostics hall is not always satisfactory due to heavy interference on a band around 300KHz, suspected to come from switching power supplies [2,3,4]. Therefore new DAQs are required to ease the diagnostic operation handling and to store more information from the JET discharges while being able to perform real-time Peak Height Analysis (PHA) for each spectral line while filtering the experiment intrinsic noise.

1.2. GAMMA-RAY SPECTROSCOPY

The gamma-ray spectrometers limitations are firstly introduced by scintillators, BGO and NaI(Tl) as they present high background noise induced by neutrons in the detector's surroundings, slow response times (limiting the maximum throughput) and low energy resolution at lower energies (for instance, NaI presents a Full Width Half Mean (FWHM) > 7% at 662keV).

NaI detectors are replaced by Lanthanum halide LaBr3(Ce) crystal (3”×6”) which accomplishes very good resolution at lower energies (less than 3% at 662keV), excellent timing resolution, high light efficiency and insensitivity to neutrons. This scintillator is coupled to a Hamamatsu Photo Multiplier Tube (PMT) designed to allow operations at rates up to 2MHz [5].

To cope with this time resolution, DAQ systems must be able to perform acquisitions at very high rates and must also have the processing capability to discriminate only the relevant events. This feature is crucial in order to scan the whole discharge time while being able to build a real time spectrum and resolve piled-up events.

The following chapters present a brief description of the DAQ system, its processing capabilities, the calibration processes necessary to adjust all the parameters before a pulse discharge and concludes with some results from two diagnostics JET pulse discharges and also from high throughput experiments outside JET.

2. DATA ACQUISITION AND PROCESSING SYSTEM

The new data acquisition solution is based on the Advanced Telecommunications Computing Architecture™ (ATCA) specification PICMG 3.0, on the PCI Express™ (PCIe) fabric PICMG 3.4 link-layer protocol [6, 7]. Each system is composed by an ATCA crate, one central controller and up to 5 Transient Recorder and Processing (TRP) modules. A TRP module contains 8 acquisition channels with 14-bit resolution, and maximum sampling rate of 400MHz. This rate is configurable

in the firmware and can be set to a different value whenever required [8].

The central controller is based on a standard ×86 motherboard with an Intel Quad® processor [9]. It uses PCIe ×1 links to coordinate the connection between the different acquisition modules and the processing unit, being responsible for the configuration and data retrieval from the TRP module memory. The boards are enclosed in a 14-slot ATCA shelf (sub-rack).

A TRP module contains two acquisition blocks, each with its own controller and PCIe endpoint, provided by a Xilinx®, virtexTM 4 family (XC4FX60) field programmable gate array (FPGA). Clock distribution and memory are also independent in each block [8].

Figure 1 depicts the path from the acquisition of the signals to the final JET data archiving. The hardware block includes the real time processing capabilities, such as triggering, segmentation, PHA and pile-up resolving. The bridge to the operating system is performed using a device-driver, translating the higher level software requests to the appropriate PCIe commands. A generic C++ interface provides the connection between the device driver and the higher level FireSignal (FS) node [10]. This node bridges the JET Control and Data Acquisition System (CODAS) to the diagnostic, preparing the diagnostic before the plasma pulse, for the configurations provided by the user (e.g. acquisition frequency, input filters parameters and number of samples). It is also responsible for providing a state machine synchronized to the JET environment, triggering the acquisition and data collection at the correct times. Upon pulse termination data is collected by the JET archive and stored in the databases as Late Pulse Files (LPF).

3. PROCESSING CAPABILITIES

The first problem, addressed by the diagnostics needs of DAQ systems, is related to the high acquisition rate that without any processing (raw data acquisition mode) would fill up the available memory very quickly, either on-board or in databases in real-time acquisitions. The second problem is related to the foreseen long-duration plasma discharges in magnetic fusion devices.

The full processing capabilities aren't always the better option for specific experiment as only an energy value is stored with the respective timestamp. As referred before, storing raw data also has its limitations, so it is required some pre-processing capacities capable of identifying events of interest, through event segmentation storage and adaptative calibration (several parameters can be easily changed by the operator before an experience run), where the validation of an event must be consistent with the real-time frame. This pre-processing is implemented in programmable logic described in Hardware Description Language (HDL).

3.1. SEGMENTATION

The current real-time processing capabilities include advanced triggering modes used for segmentation purposes and events (segment) validation. After an event being detected and before starting to be stored at memory, the segment is subjected to an event evaluation. This evaluation is critical for the gamma-camera diagnostic as it includes noise in the same bandwidth, besides the

already mentioned intrinsic 300kHz interference at the introduction section. Figure 2 presents a fraction of a segmented acquisition sampled at 100MHz, during the pulse JET Pulse No: 79692, where the two types of interference and good events can be easily seen. Besides event triggering, event discriminator technique is required to decrease the amount of collected data. The triggering and event validation are showed at Figure 3.

During segmentation over each event detection, any new incoming event is neglected, that is, the system does not present dead time [11]. Every time an event occurs, a user defined number of samples (PWIDTH) are stored with an associated timestamp, setting the beginning of each pulse event for time reconstruction, thus allowing time-resolved spectroscopy.

After storing the triggered event on a temporary buffer, the system waits for another trigger. Meanwhile, if pile-up occurs, then it has to be resolved off-line. This procedure was performed using MatlabTM offline algorithms that can be later translated to HDL code.

The system allows the selection of two trigger modes: by level and by edge. In the former, a voltage level comparison is performed between successive samples and a user defined threshold value; while on the latter, a linear regression is done to the rising edge of the event. If the difference between consecutive samples is higher than a slope value, an event has occurred. This type of triggering is more accurate in respect to the level one, since it is more insensitive to time jitter. A data moving average of 2 to 8 can also be chosen, before triggering process to decrease false triggers due to signal noise, although for the gamma camera this moving average is not enough.

3.2. EVENT VALIDATION

Event or segment validation process allows to reject segments due to a false trigger (false event), or to help to detect pile-up events on a segment. Every time an event is tagged as false event (for instance, at gamma camera when the noise of the same bandwidth of events occurs, the systems triggers noise as an event) a parallel process is opened to detect if there is more than one rising edge on the triggered segment. This checking process consists on the verification of the number of consecutive incremental samples, else no pile-up had occurred and the segment contains a false event and is discarded. Only segments with validated events or with pile-up occurrences are stored in memory.

To validate a segment, firstly the segment under evaluation, d[1:PWIDTH], is baseline restored. A baseline restoration is based on an average calculation between all the pre-trigger (PTRG) samples of the segment. The calculated average is subtracted to all the samples, p[1:PWIDTH]. After removing baseline, simultaneously, the maximum amplitude value of p[1:PWIDTH] is calculated, max(i), while the trapezoidal filter is applied to the same data to retrieve the event energy value, Energy(i), where i is the number of the segment being studied. Finally, the segment validation consists on checking if the relation between Energy(i) and max(i) is higher than a user defined threshold, Figure 4. The determination of this threshold is done through calibration process.

3.3. PILE-UP

After detecting pile-up within a segment, by checking if a settled number of consecutive samples is incremental (defined by the gamma-ray rising time), the algorithm evaluates if it is possible to restore each overlapped event. This possibility depends on the number of samples describing the overlapped event.

Figure 5 shows the reconstruction of two overlapped events in a single segment. This reconstruction consists of two steps: determine the starting point of the second overlapped event and restore the baseline.

3.4. PHA

The pulse/event analysis culminates with the PHA where a pulse is resumed to its amplitude value and respective timestamp to be stored in memory. This process must pass through several tests before asserting its reliability. Special care was taken because there was too much sensitivity on the pulse shaping techniques to variations in the detector charge collection time. Ballistic deficit and charge trapping effects can noticeably reduce the resolution of spectrometers when shapers producing short pulses with sharp peaks are used. It has been demonstrated that these effects can be reduced by using flat-topped shapes [12, 13]. The relation between event rise/falling time is essential for the trapezoidal filter application. These two parameters are dependent of the experimental apparatus (PMT and detector). When the ratio between rising time and falling time is higher than 0.1 the filter output doesn't present a flat top, instead it is much similar to the pulse itself. With the absence of a flat top the last sample related to the flat top cannot be taken into account and instead the maximum value of the filter output is considered. The result of this trapezoidal filter adaptation is presented in the graphics of the results section. The reasons to use this kind of trapezoidal filter are i) It is already implemented at FPGA environment [9, 14]; ii) Amplitude of the shaped pulse is independent of any DC offset of the input signal; iii) Avoidance of resolution loss due to ballistic deficit, with an appropriate trimming of the filter parameters.

4. CALIBRATION

The system is able to acquire data on raw mode, segmented mode, segmented validation mode and PHA mode. The first two modes are of crucial importance for system calibration. The raw mode is used to settle the threshold value for triggering, the segmented mode is used to settle the threshold value for segment validation and fit the pulses to a reference in order to set the rising/falling time for the trapezoidal filter parameters. The last two modes are the final operational modes.

5. RESULTS

This section shows the two diagnostic results during two different pulse JET discharges. Gamma-ray emission is caused by reactions between fast particles and fuel ion or more frequently with impurities such as carbon and beryllium. Two major sources of fast ions, presented at the two

discharges, are the injection of neutral beam ions (NBI) with energies usually of the order of 50 to 150keV and acceleration of ions via ICRH [2,5].

Some tests with the full system (detector + PMT + DAQ) were also performed outside JET to study the system response to high count rates experiments and to understand which rate the processing algorithm can handle to build a spectrum and to clarify the worsening of the peak lines resolution when compared to values obtained at low rates. High rate gamma spectroscopy measurements were held at Ioffe cyclotron ion beam at St. Petersburg and at the Tandem Van Der Graaf accelerator of Magurele-Bucharest. It should be stressed that the current results are preliminary but represent the first effort to accomplish real-time analysis. For the GRS diagnostic there are enough channels to duplicate the acquisition paths in order to have real-time results to compare with the offline and more accurate results. This scenario is not feasible in the gamma camera since it hasn't enough available channels to duplicate the inputs. To overcome the lack of input channels a simultaneous operation mode, where data is being processed and streamed in real-time while filling the on-board memory with raw data, allows off-line validation of the processed data and a continuous operation of the diagnostic [15].

5.1. GAMMA CAMERA RESULTS

The results presented at Figure 6 were taken with the detectors being in shadow position (does not have a direct line-of-sight to the plasma). Only one channel was provided for the experiment (vertical camera (channel 14)), in order not to interfere with the operation of present gamma-camera diagnostic. A delay period, relative to the JET pulse start time, was set to the start of the acquisition in order to obtain the regions of interest, where the Neutral Beam Injection (NBI) and, if existent, the ICRH time windows are present. For each discharge all data was acquired in segmented mode with different configurations.

Figure 6 depicts the gamma-ray distribution of Pulse No: 79692. This pulse was chosen among others because it has more events due to the presence of ICRH. Events were quite sparse having a maximum of occurrence during NBI and ICRH time windows. The following conclusions can be taken: i) Due to interferences with the same bandwidth of the gamma-ray pulses, real-time event validation is mandatory; ii) For the given line of sight (channel 14) the background was significantly low, meaning very few gamma-ray reactions; iii) Although very sparse, gamma-ray reactions occurred during NBI/ICRH time window, the system is acquiring properly; iv) Additional tests with the 19 DAQs channels are required .

5.2. GAMMA-RAY SPECTROSCOPY RESULTS

5.2.1 Cyclotron ion beam

Tests to perform high gamma spectroscopy for the reaction $^{9}Be(\alpha, n\gamma)^{12}C$ were available at cyclotron ion beam at Ioffe Institute with the following experimental conditions: $^{4}He^{+}$ ions were accelerated to 5.3MeV irradiating a thick beryllium target. The cyclotron duty cycle period was 10ms and

within each duty cycle the alpha beam could hit the ^{9}Be target for 1 to 9ms.

The DAQs was operated at raw mode, at 200MHz., because at the time of the experiment, the system did not perform data segmentation. A file with the acquired raw data was provided in order to run the offline processing routine, based on the trapezoidal algorithm. This was done to prove if the same algorithm as the one running inside the FPGA, could handle the bursts of gamma-ray reactions and be able to build a spectrum where the calibration lines (^{137}Cs and ^{60}Co) as well as the reaction lines ^{9}Be(α, n γ)^{12}C could be clearly distinguished.

Figure 7 shows gamma-ray spectrum obtained by bombarding a thick beryllium target with α beam of 5.3MeV during 2ms. The calculated relative peak resolution was of 3.9% for ^{137}Cs, comparing to the % obtained in ideal conditions (no noise, laboratory conditions, optimized analog chain).

5.2.2 Tandem accelerator IFIN-HH

Intense gamma-ray and neutron sources were available at tandem accelerator of IFIN-HH, Magurele-Bucharest. To obtain such conditions, an aluminum target was irradiated with a 10MeV proton beam. The following energy lines are focused and depicted at Figure 8: i) 843keV and 1014keV obtained from the reaction ^{27}Al(p,n)^{27}Si. The half life for the nucleus ^{27}Si is of 4.16 s and its decay feeds the transitions of the nucleus ^{27}Al; ii) ^{27}Si decay by the predominantly β+ emission, producing a strong 511keV annihilation peak; iii) 1368keV gamma-ray was obtained from the reaction of ^{27}Al(p,α)^{24}Mg [16]; iv) there are three calibration lines:1) 662keV from ^{137}Cs calibration source, 2) 1458keV (^{138}La) from the intrinsic detector radioactivity and 3) a high energy line from a control and monitoring system based on two independent Light Emitting Diodes (LED) which send light pulses via optical fibers to the PMT photocathode for calibration purposes [5]. These calibration lines are only visible at the low rate spectrum, because gamma-rays emitted by calibration sources and by the intrinsic detector radioactivity need a certain time to have enough statistics to appear as well defined spectral lines. DAQ system memory is written every time an event occurs and this writing process ends if the memory is full, or by software after a defined time (for instance, after a JET pulse discharge). During high throughput experiments the memory is full before the experience run time.

Figure 8 evidences the difference between the 2 acquisitions one with a high count rate, 1.3 MHz, and another with lower count rate, 36kHz. These two spectra show the pile-up resolving and although the peak resolution decreases with higher gamma-ray rates, the algorithm still distinguishes all the energy lines of interest.

The DAQ system was operated at segmented mode at 400MHz, triggered by level.

5.2.3 JET pulse discharges

The data presented at Figure 9 was taken during the intensive gamma radiation intervals of the JET pulse discharges by DAQ system. The aim of the JET Pulse No: 79174 experiment was to accelerate alpha particles to study fast ions physics. The alpha particles were injected as beams and then

accelerated by radio-frequency to increase their energy. Gammas from the reaction $^{9}Be(\alpha, n\gamma)^{12}C$ were expected as well as gammas from the reaction ^{12}C (d, p γ) ^{13}C are evidenced at the spectrum. If a JET pulse discharge without ICRH was presented, only the calibration lines along with the intrinsic detector radioactivity would be showed.

The DAQ system was equally operated at segmented mode at 400MHz, triggered by level.

CONCLUSIONS

A DAQ real-time processing system for plasma diagnostics at the JET facilities is presented. This system is used to perform the diagnostics of fast ions in fusion plasma, both through GRS and gamma-camera analysis. A brief presentation of the system is followed by the algorithms description and coarse structure, with a more in-detail discussing of its processing blocks (segmentation, pulse validation, pulse height analyzer and pile-up processor).

Tests were performed with data from both analyses, at high count-rates, to extensively assess the processing algorithms performance. The presented results reveal a very good performance for the segmentation and validation algorithms as well as the pulse height analyzer efficiency. Pulse pile-up processor was given special attention due to its importance on the final spectral resolution at very high count rates. Results show that a satisfactory performance is accomplished at these high throughputs but still far from the resolutions obtained for low event rates. This fact reveals the need for the algorithm optimization to comply with the real-time processing nature which will be determinant for very high throughput measurements, such as those of ITER burning plasmas.

FUTURE WORK

For gamma-camera diagnostic tests must be performed with the 19 channels in order to have all channels tested on-site (JET) in parallel with the old gamma/neutron camera system and with radioactive sources.

For both diagnostics, the pile-up rejection/resolving must be implemented at FPGA and tested during JET pulses discharges.

The real-time PHA although not used during JET pulse discharges has already been tested on-site and has properly worked when pulses presented a rising edge much faster than the falling edge. A small modification to the filter algorithm has been introduced, where instead of using the last point of the trapezoidal flat top output as the event energy, the maximum value of the output is taken into account. Further tests must be done to validate this operation mode.

REFERENCES

[1]. Saoutic B. 2002 Plasma Physics and Controlled Fusion **44** 1–12;

[2]. V.G. Kiptily F.E. Cecil and S. Medley, “Gamma-ray diagnostics of high temperature magnetically confined fusion plasmas”,Plasma Physics and Controlled Fusion, **48**, (2006), R59-R82;

[3]. V.G. Kiptily, F.E. Cecil, S.S. Medley et al., Nucler Fusion **45**, L21 2005;

[4]. JET-EP2 - Project Management Plan: "DAQ for gamma diagnostics", 2009, JET internal document. This document can be requested to ritacp@lei.fis.uc.pt

[5]. M. Tardocchi et al, "Gamma ray spectroscopy at high energy and high time resolution at JET", Review of Scientific Instruments, vol **79**. 10E524, 2008;

[6]. AdvancedTCA®, PICMG® 3.0 Revision 2.0, AdvancedTCA® Base Specification, March 18, 2005;

[7]. www.pcisig.com;

[8]. R.C. Pereira, J. Sousa, A.M. Fernandes, F. Patrício, B. Carvalho, A.Neto, C.A.F. Varandas, G. Gorini, M. Tardocchi, D.Gin, A. Shevelev, "ATCA Data Acquisition system for gamma ray spectrometry", Fusion Engineering and Design, Vol **83**, IS 2-3, pg:341-345, 2008;

[9]. A.J.N. Batista, J. Sousa, and C.A.F. Varandas, "ATCA digital controller hardware for vertical stabilization of plasmas in tokamaks,"Review of Scientif Instruments, Review of Scientific Instruments **77**, 10F527 (2006);

[10]. A. Neto, J. Sousa, B. Carvalho, H. Fernandes, R.C. Pereira, A.M. Fernandes Varandas, G. Gorini, M. Tardocchi, D. Gin, A. Shevelev and K. Kneupner, "The control and data acquisition software for the gamma-ray spectroscopy ATCA sub-systems of the JET-EP2 enhancements" Fusion Engineering and Design, Vol **83**, IS 2-3, PG:346-349, 2008;

[11]. João M. Cardoso, J. Basílio Simões and Carlos M. B. A. Correia, "Dead Time Analysis of Digital Spectrometers", Nuclear Instruments and Methods in Physics Research A **522** (2004) 487-494;

[12]. V.T. Jordanov, Glenn F. Knoll, "Digital synthesis of pulse shapes in real time for high resolution radiation spectroscopy", Nuclear Instruments Meth. Phys. Res., vol. 345, pp. 337-345, 1994;

[13]. V.T. Jordanov et all, Digital techniques for real-time pulse shaping in radiation measurements, Nuclear Instruments and Methods in Physics Research A **353** (1994) 261–264;

[14]. A.M. Fernandes, R.C. Pereira, J. Sousa, A. Neto, P. Carvalho, A.J.N. Batista,B.B. Carvalho, C.A.F. Varandas, M. Tardocchi, G. Gorini and JET EFDA contributors, "Parallel Processing Method for High Speed Real Time Digital Pulse Processing for Gamma-Ray Spectroscopy", Journal of Fusion Engineering and Design, in press;

[15]. R.C. Pereira, A.M. Fernandes, J. Sousa, J. Cardoso, C.M.B.A. Correia, M. Tardocchi, M. Nocente, G. Gorini, V. Kiptily, B. Syme, M. Jennison and JET-EFDA contributors, "Pulse analysis for gamma-ray diagnostics ATCA sub-systems of JET tokamak", IEEE Transactions in Nuclear Science, in press;

[16]. http://www.ifa-mg.ro/euratom/Documentatie/raports/2007/cap_3b.pdf

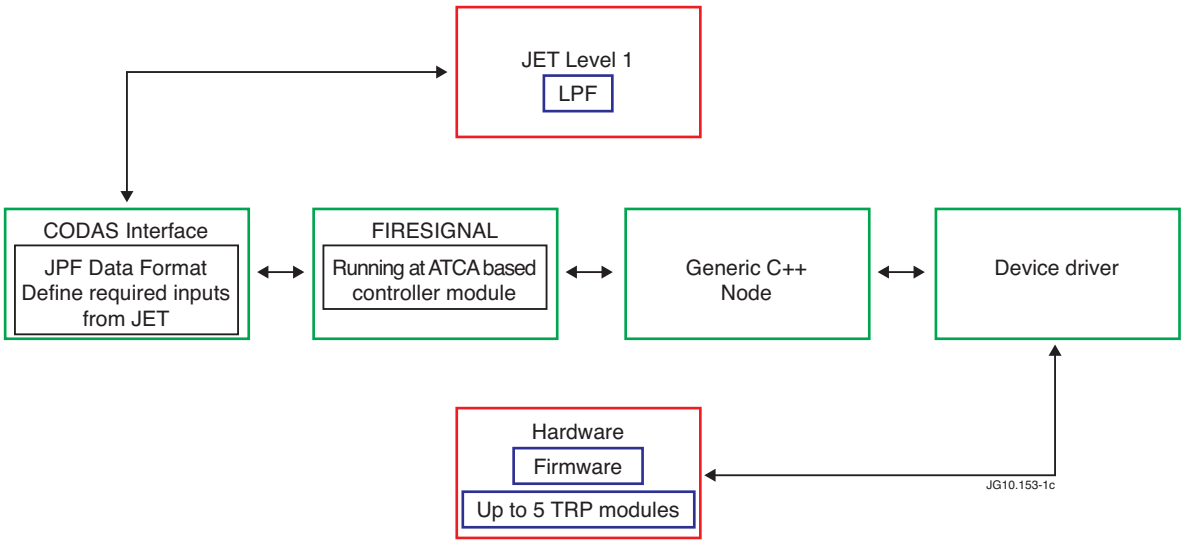

Figure 1: Data acquisition system diagram flow

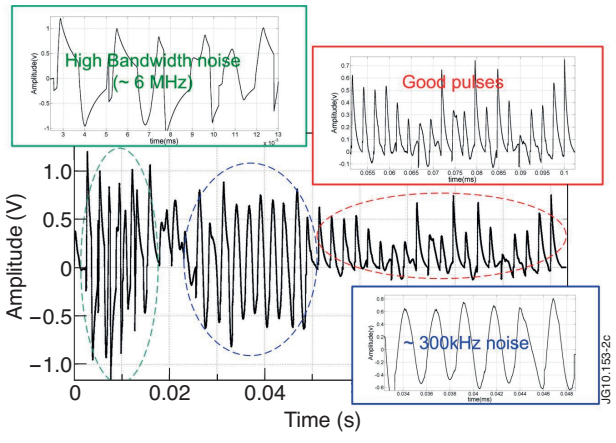

Figure 2: A piece of acquisition of the JET Pulse No: 79692, showing the low and high bandwidth noise.

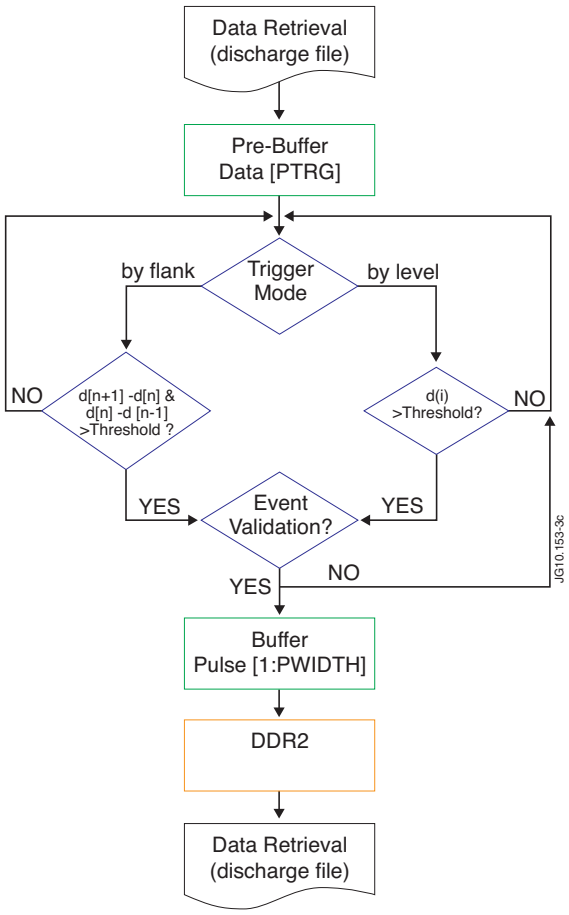

Figure 3: DAQ system segmented data operation mode flowchart. A number of PTRG of samples are always being stored at a pre-buffer. Then a trigger mode is chosen by the operator to allow event detection. If an event is detected (triggered), follows its validation process. After validation, the data segment of the size of PWDITH samples is stored at on-board memory.

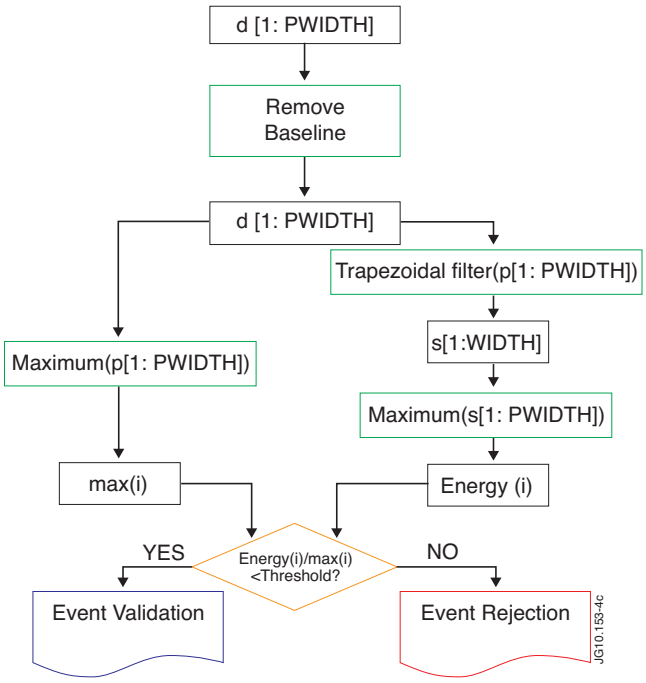

Figure 4: Event validation flowchart.

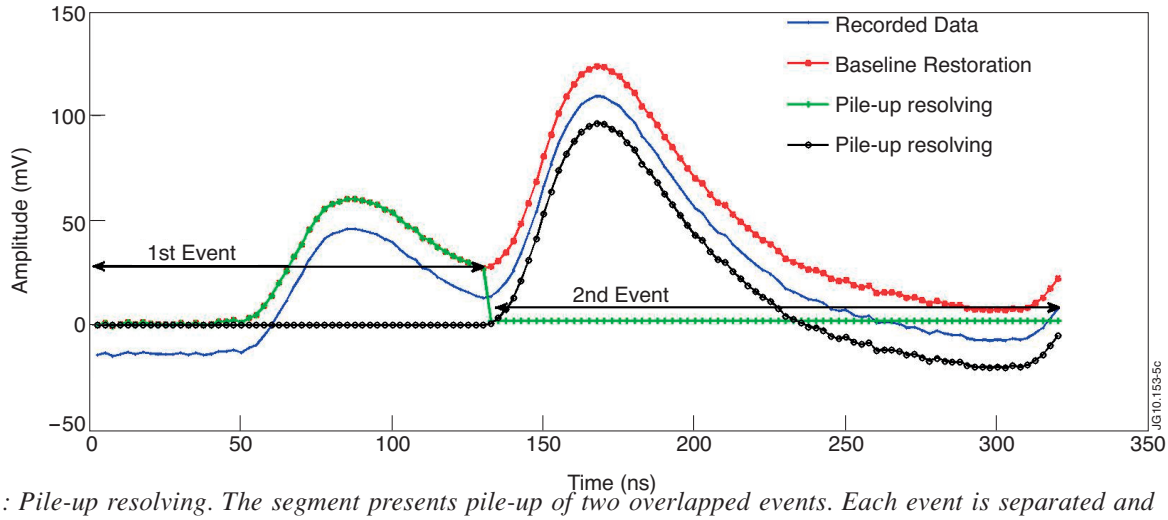

Figure 5: Pile-up resolving. The segment presents pile-up of two overlapped events. Each event is separated and reconstructed.

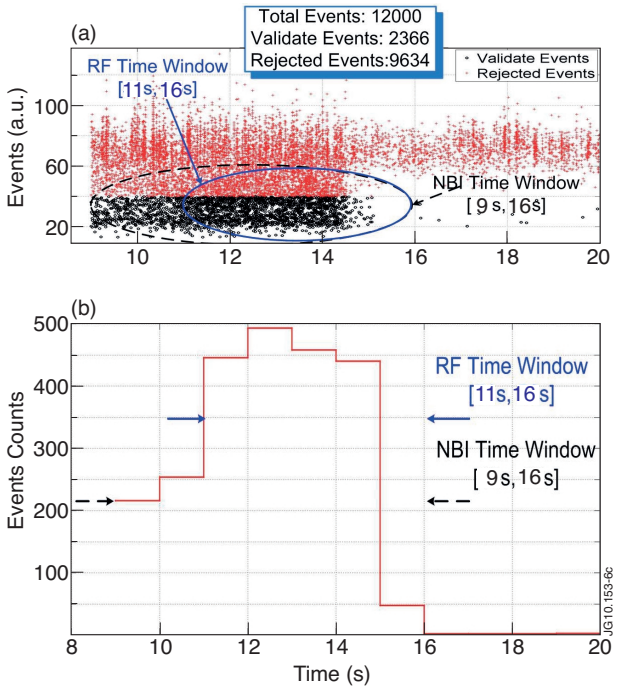

Figure 6: Events distribution of Pulse No: 79692: a) Relation between event validation and the JET pulse discharge time window; b) Gamma-ray rate versus JET pulse discharge time window.

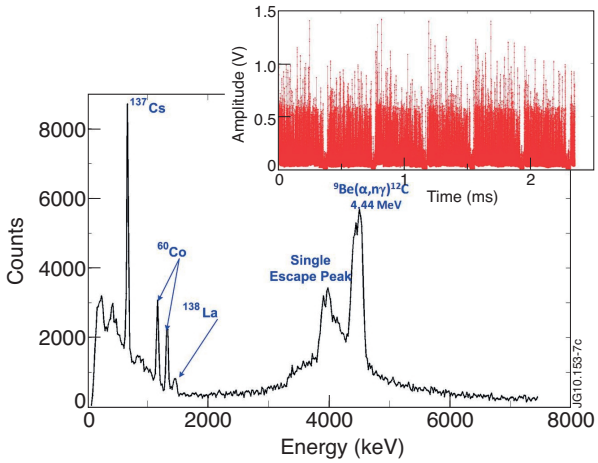

Figure 7: Gamma-ray spectrum obtained by bombarding a thick beryllium target with a beams of 5.3MeV. Gamma-rays occur in bursts depending on the 10ms cyclotron duty cycle period and within this period, depending on the time duration of the a beam target hit of 2ms.

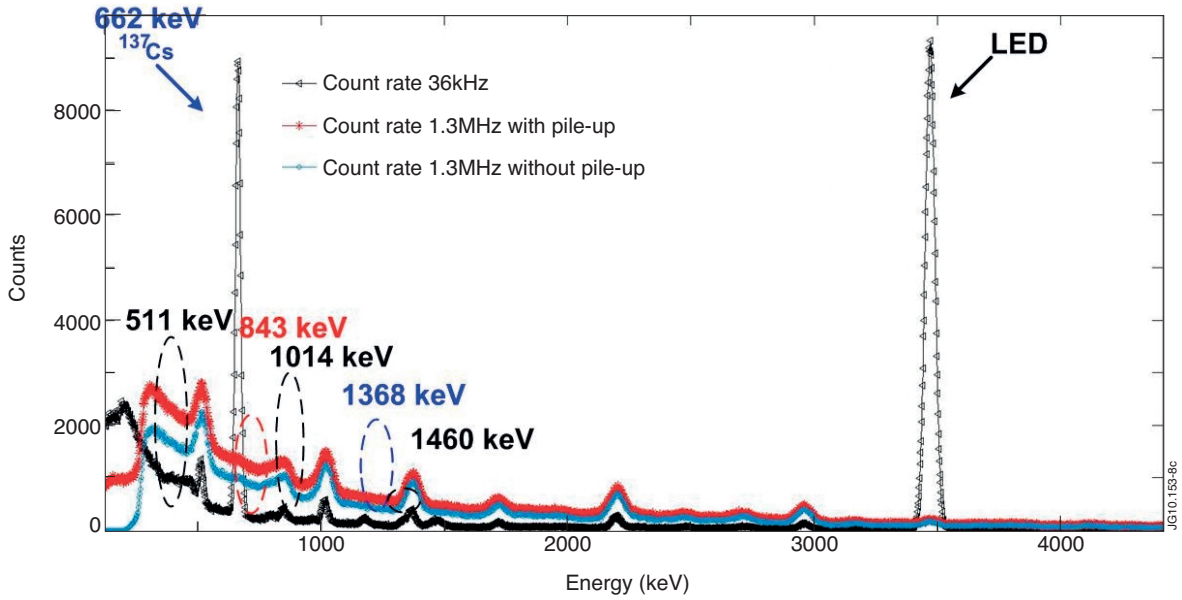

Figure 8: Gamma-ray spectra obtained by bombarding an aluminum target with a proton beam of 10MeV, with a reaction rate of 1.3MHz and 36kHz.

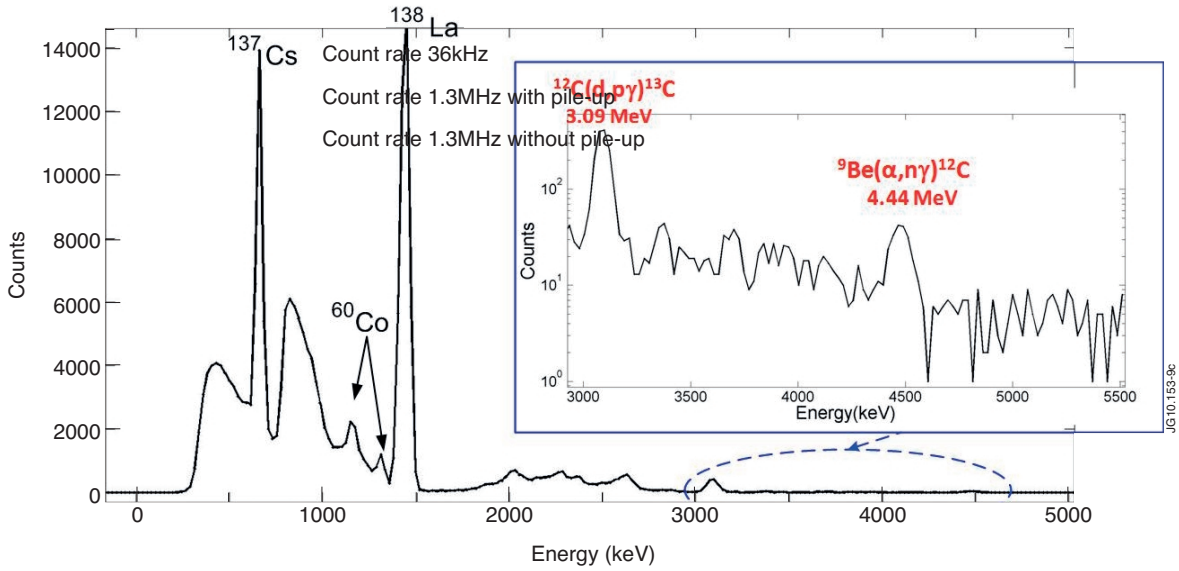

Figure 9: Gamma ray spectrum from JET Pulse No: 79174 obtained with the DAQs and the offline processing. Gamma ray lines due to the $^{12}C(d, p\gamma)^{13}C$ and $^{9}Be(^{3}He, p\gamma)^{11}B$ reactions can be clearly seen at the high energies . Other lines can also be seen due to calibration sources (^{137}Cs and ^{60}Co) or intrinsic detector radioactivity (^{138}La).